

INFLUENCE OF THE SPUR DIKE PERMEABILITY ON FLOW AND SCOURING DURING A SURGE PASS

Tomasz MIODUSZEWSKI

Graduate School of Natural Science and Technology, Okayama 700-8530, Japan,
E-mail: tomasz@cc.okayama-u.ac.jp

Shiro MAENO

Dept. of Civil Engineering, Okayama University, Okayama 700-8530, Japan,
Tel. (+81) 86 251 8151, fax (+81) 86 251 8257
E-mail: maeno@cc.okayama-u.ac.jp

Yatsugi UEMA

Dept. of Civil Engineering, Okayama University, Okayama 700-8530, Japan,
E-mail: ev15013@cc.okayama-u.ac.jp

Abstract: An experimental look on the influence of the structure permeability on flow pattern and local scouring process near a spur dike is presented in this paper. Detailed measurements of pressure and scouring action, performed in cases of permeable and impermeable structure, gave materials to compare such parameters as water level, excess pore pressure, seepage force and final scour profile. Significant differences among cases were noticed in all those factors. The permeability of the spur-dike was recognized as a very important feature that results in preserving the riverbed from scouring. The values of all other parameters which may promote scouring were noticeably smaller. The experiments were conducted simulating conditions of a surge flow, which additionally exposed all measured parameters. The disaster-like type of flow showed very significant differences between two examined types of spur dikes.

Key words: Spur dike; permeability; Hydrodynamic pressure; Excess pore pressure; Liquefaction; Seepage force; Surge flow; Scouring.

1. INTRODUCTION

Spur dikes are the most important river training structures. The main reasons for their usage are redirecting the flow of water and preserving the desired depth of a river or channel. Diversification of the flux is also a very important goal for spur dike planning. Another application, since a system of spur dikes may protect riverbanks, is strictly connected with landscape formation. From this point of view the dike itself is a part of scenic environment and its appearance is very important. Because of the big number of various goals of application, different parameters have different levels of importance in choosing the structure type.

A number of investigations were performed to improve understanding the flow phenomena around dikes. At the beginning it has to be said, that all structures investigated before were



Photo 1 Stable flow around spur dike

impermeable. Most of the researchers focused on the scouring depth and velocity of a stable flow. Those two factors as well as the stability of structures are crucial parameters for the spur dike application. A study on velocity profiles and scouring process in the vicinity of submerged dikes were performed by Elawady et al. (2000, 2001) and Rahman et al. (1998). A similar subject i.e. scouring around coastal structures under action of waves and currents, which is, in general, the same phenomenon, was investigated by Summer et al. (1994, 2001) and published in many papers.

Nevertheless, other factors are supposed to influence the scouring phenomenon. In this study the influences of excess pore water pressure, seepage force and liquefaction were examined. Those parameters were investigated in the past by researchers in other cases of structures. For example Mia (2002) has studied influence of liquefaction induced by the flow on bridge piers. Many scientists still take the earthquake- induced liquefaction into consideration. The wave-induced liquefaction is also described in many works. The rules governing those phenomena caused by cyclic-loading are slightly different from those considered in this work, and will not be investigated here.

The main goal of this work is to indicate the influence of the structure permeability on flow behavior and local scouring process. Factors like excess pore pressure, seepage force and liquefaction will also be compared among the cases of permeable and impermeable structure.

2. OUTLINE OF THE EXPERIMENT

2.1 EXPERIMENTAL SETUP

Experiments were conducted in the laboratory flume of Okayama University. The laboratory flume is a 15 m long, 0.6 m wide and 0.4 m deep steel construction with its front wall made of glass. The channel inclination was 1/500. The pit for experimental installation is located in the middle part of the flume (see Fig. 1). The depth of the pit is 17 cm and its length is 100 cm. Its width is equal to the channel width. During the experiment, the pit was filled with movable sand. The sand used for this experiment is characterized by an average grain diameter $d_{50} = 1.28$ mm.

Two types of the spur dike were used in this experiment (Photo 2). The first structure was solid which is made of Plexiglas. The second one was made of steel mesh filled with stones (average size 2 cm). In both cases the spur dike was constructed as a full height

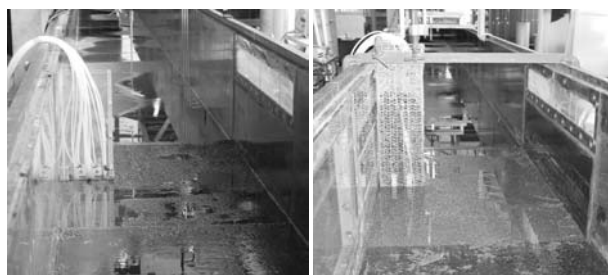


Photo 2 Experimental spur dikes

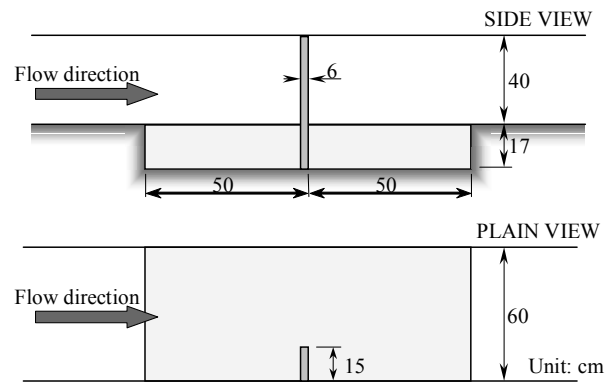


Fig. 1 Experimental setup

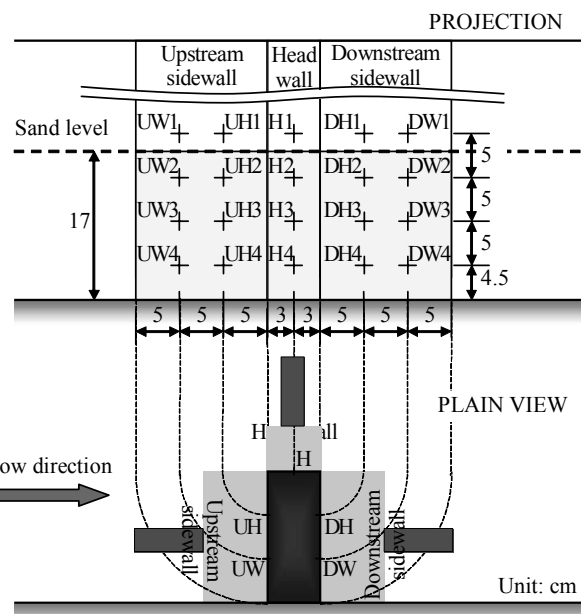


Fig. 2 Pressure sensor location

structure, 6 cm thick and 15 cm wide. As shown in Fig. 2 twenty pressure sensors were placed on it: eight on the upstream sidewall, four on the head wall and eight on the downstream sidewall. Pressure sensors were configured into five vertical columns and four horizontal rows.

The highest level of the sensors during all the experiments was above the ground level. The second and third rows from the top in some cases emerge in the water during the surge while the lowest row of sensors was still in the sand.

All pressure sensors used in the experiment were the transducer type. The sensors were connected to the amplifiers and to the computer to record the data. Sampling frequency was set to 50 Hz.

Measurement was performed at 240 s with the first 10 s as the stable flow time without initializing the surge. Those 10 seconds at the time of data analysis were used in adjusting the time scale of all cases and in adjusting the zero value at the beginning of each case and data channel. In the graphs, this time delay is not shown to make them clear - time zero indicates the opening of the gate.

Because of the big number of pressure sensors, and the video recording using the foil, each experimental case was conducted several times. The obtained results were fitted with time scales to give a uniform image of the phenomena. The videos of scouring process were time adjusted using simultaneously recorded audio track where the time of opening the gate was recorded.

The scour depth during the surge was recorded using underwater camera submerged near the dike. For purposes of recording, in the impermeable-structure case, the surface of the walls was covered by the special foil with the chessboard-type pattern. It allowed a precise measurement of the scouring depth during video postproduction process. In the permeable-dike case it was not necessary because the rods of the steel mesh were used as an indicator of the scouring progress.

2.2 HYDRAULIC CONDITIONS

The dynamic flow was chosen as a subject of the experiments. During this type of flow all processes occur more rapidly than in a stable flow. This flow pattern may be assumed as an emergency or as a breakdown situation. It is a good purpose, therefore, to conduct investigations because one breakdown might be a reason for a chain reaction of other breakdowns.

The experimental wave came from the downstream side of the dike. The surge was generated by opening the gate located at the end of the channel. Investigations were performed with the initial water depth 30 cm. The depth of the water after the experiment was stabilized at the level of about 5 cm. In both cases the water discharge was set to the value $Q = 0.005 \text{ m}^3/\text{s}$. The Froude number of the flow varied from 0.02 to 0.24.

3. EXPERIMENTAL RESULTS

3.1 PRESSURE CHARACTERISTICS

Pressure characteristics are shown in Fig. 3 and 4 for permeable and impermeable structure respectively. In all pressure figures presented in this paper, one can see only alterations of the pressure. At the beginning of each run the value of the pressure in every point was set to the value zero. This allows comparing all the lines without considering the hydrostatic pressure. What is more, considering good legibility, the time axis in all pressure figures was truncated to only 40 seconds, neglecting the first 10 s of stable flow used only for time adjustment.

At the beginning of each recording one can see about 3 seconds of oscillating pressure. It is supposed to be the effect of the process of opening the gate. This assumption is confirmed by the fact that, during these oscillations, the average value of the pressure was not changing. Other parameters (like water depth and velocity) also during this time remained unchanged.

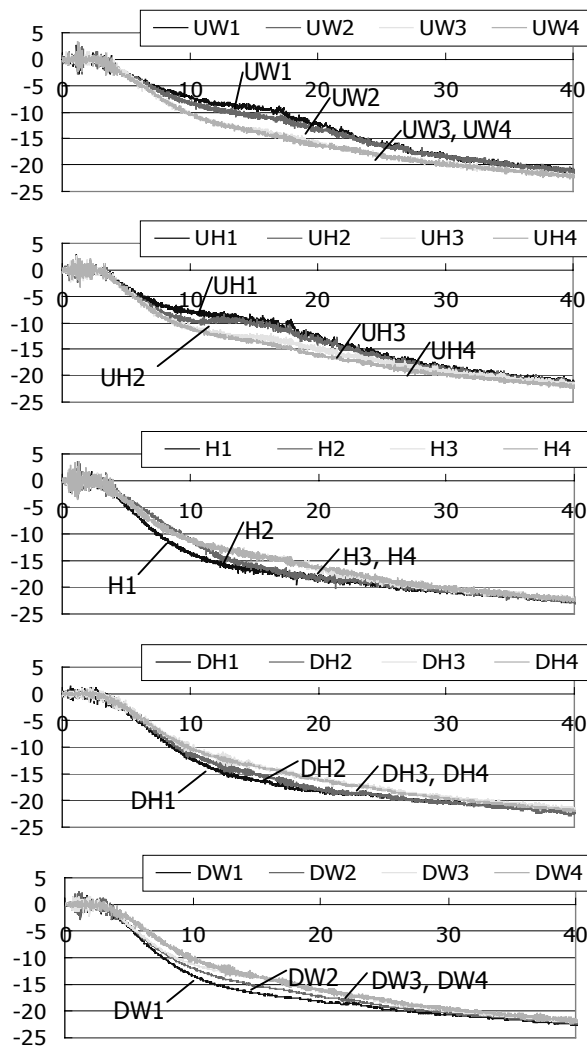


Fig. 3 Pressure characteristics (unit: cm) permeable structure

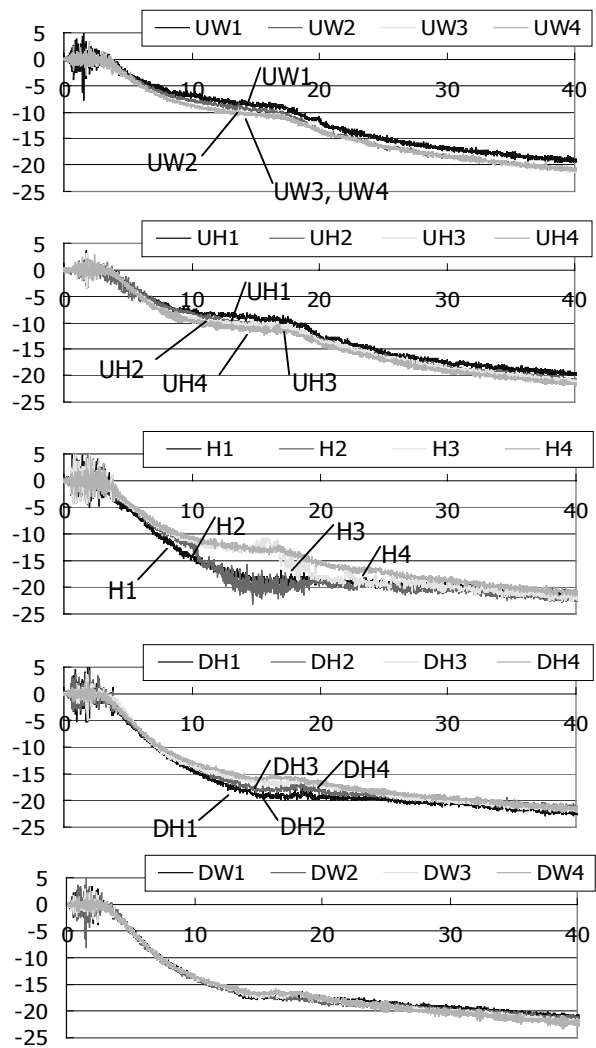


Fig. 4 Pressure characteristics (unit: cm) impermeable structure

This oscillation is seen in all runs, in both cases - for the permeable and impermeable structure what is also a proof, that it is connected with an experimental procedure.

Generally speaking the pressure change tendency corresponds with the change of water level. For points placed above sand level both, the value of pressure and the water level changes simultaneously. The change of pressure in different columns occurs in slightly different way. The pressure changes most rapidly at the downstream sidewall. Water level near the upstream sidewall falls down less rapidly which is the reason for the steady decrease of the pressure value. Comparison between cases with and without permeability shows noticeable distinction in pressure change pattern. In the permeable structure case the change is characterized by a more constant decrease. Difference between upstream-side and downstream-side is also smaller (see Fig. 5). While in case of impermeable structure the maximum pressure level alteration between upstream and downstream side is about 9 cm, in the case of permeable structure the same value equals 7.8 cm. Maximum difference between cases is equal 1.5 cm. The reason

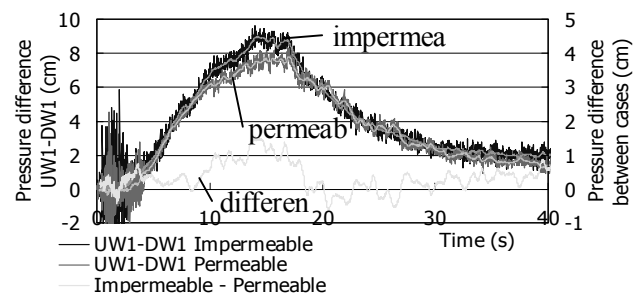


Fig. 5 Pressure difference – downstream/upstream

for this is the possibility of water flow through the permeable structure.

Pressure in the sand shows a kind of delay in changing pressure in the lower layers in the sand alternate much slower than in the upper layers. The biggest difference in pressure change at specified layers is visible in the H column in the case of impermeable structure. This phenomenon is a reason for the appearance of excess pore pressure.

3.2 EXCESS PORE PRESSURE

The excess pore pressure graphs for permeable-structure and impermeable-structure case is presented in Fig. 6 and Fig. 7 respectively. Pressure sensors located above the sand level have measured the total pressure in a column - namely the hydrostatic and hydrodynamic pressure. Because of the rapid changes in the pressure above the sand, the pressure measured in the sand showed some difference according to the limited velocity of water flow in the sand layer. The observed difference of pressures between values in the sand and above it is an excess pore water pressure. For each point in the sand, where pressure measurements were conducted, the excess pore water pressure was calculated as a difference between the pressure value at this point and at the point located in the water above the sand in the same column. Usage of this method of calculation results in a considerably small error because the comparison is done between two pressure values located in the same column.

The highest level of excess pore water pressure is in column H for the case of impermeable structure. The biggest difference between pressures above the sand and in the layer of sand is in column H (Fig. 4). The pressure measured in the point above the sand is changing most rapidly, while the pressure measured in the sand layer is changing quite slowly (Fig. 3 and Fig. 4). Similar pattern is visible in the pressures recorded at the downstream sidewall of the spur dike. As a result, the excess pore water pressures in those columns have big positive values (Fig. 6 and Fig. 7). It means that the pressure in the ground is bigger compared to the pressure in the water. This pattern is valid for both cases. Nevertheless the excess pore pressure in the permeable-structure case is noticeably smaller in all columns. A slightly different situation was recorded at the upstream sidewall. It is because not only the change of the pressure is slower but also the hydrodynamic pressure acts on this sidewall so that the pressure in the water changed slower than in the sand. For the impermeable-structure case, the difference is almost insignificant but the graph for the upstream sidewall shows a small negative value of excess pore water pressure (Fig. 7). For the permeable-structure case the pressure difference is rather significant and, in Fig. 6, one can see almost as big negative excess pore pressure for the UH column as positive pressure for H column.

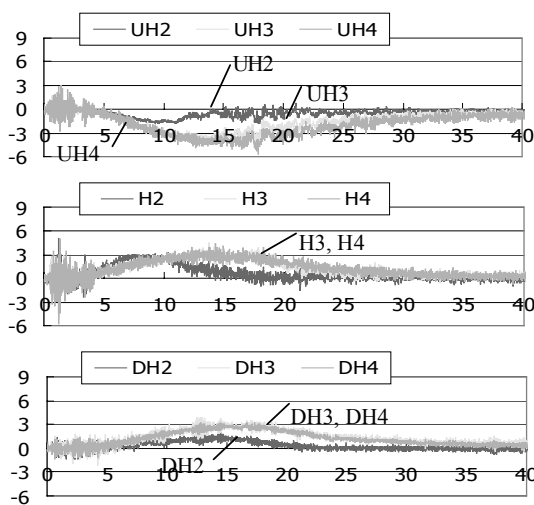


Fig. 6 Excess pore pressure (unit: cm) permeable structure

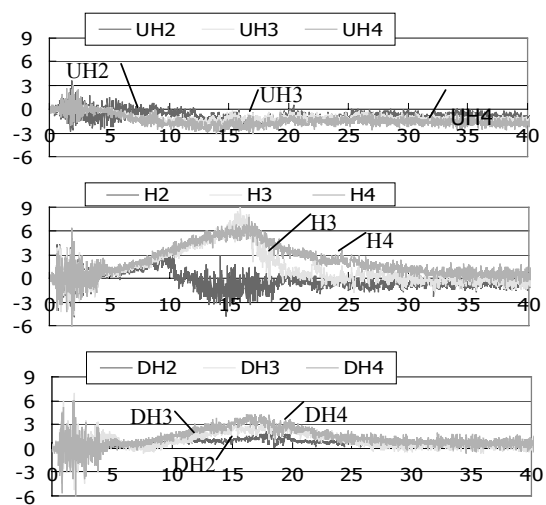


Fig. 7 Excess pore pressure (unit: cm) impermeable structure

3.3 LIQUEFACTION

Usually the occurrence of excess pore water pressure is accompanied by the liquefaction process. The equation that allows calculation of the dimensionless effective stress at specified depth in the sand according to the scour depth and the excess pore water pressure was proposed by Nago (1981) on the experimental basis:

$$\sigma_z = 1 - \frac{\rho_w \cdot g \cdot h'}{(\rho_s - \rho_w) \cdot g \cdot (Z - z) \cdot (1 - \lambda)} \quad (1)$$

where σ_z is the dimensionless effective stress; h' is the excess pore water pressure; g is the acceleration due to gravity ρ_s and ρ_w are the sand and water density, respectively; z is scouring depth above the point of calculation; Z is the initial sand layer thickness above the point of calculation and λ is the porosity of sand.

In this article, effective stress was calculated for several points arrayed at the spur dike according to Eq. 1. Results are presented in Fig. 8 and Fig. 9 for permeable-dike and impermeable-dike case respectively. In those graphs, the vertical lines with arrows show the moment that points emerged in water. The identification of the emerging point is indicated inside arrows.

The liquefaction process near the specified point happens as the dimensionless effective stress calculated for this point decreases to the zero value while the point is still submerged in the sand. The liquefaction process takes place or almost all points that emerge in the water at the headwall and downstream sidewall. At the upstream sidewall the liquefaction process was not observed because the excess pore water pressure has a negative value. The time of liquefaction varies in different points. The times of the liquefaction processes are presented in Table 1.

Table 1 Times of the liquefaction in points (unit: s)

	permeable dike	impermeable dike
H2	3.16	1.12
H3	1.98	3.42
H4	-	7.04
DH2	7.00	5.10

The longest time of liquefaction is seen for the points located at the downstream sidewall. In the permeable-dike case, near point DH2, the sand is liquefied for the longest time, but this point does not emerge in water. The same point in the impermeable-dike case is also characterized by the longest liquefaction time. In both cases the final scour level is very close to this point. Because it is in the "border layer" the liquefaction time is the longest. The sand near points H2 and H3 was also liquefied but for a shorter time. The vicinity of headwall is the area where all processes have the most rapid run. In this column the observed liquefaction is the deepest among others. In the case of impermeable structure even in point H4 (initially 12.5 cm below sand level) the liquefaction phenomenon was observed. It lasted over 7 seconds. After that time, effective stress gradually reached the initial value. In the vicinity

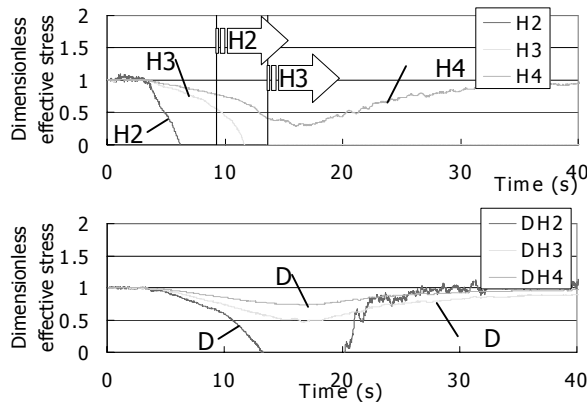


Fig. 8 Dimensionless effective stress permeable structure

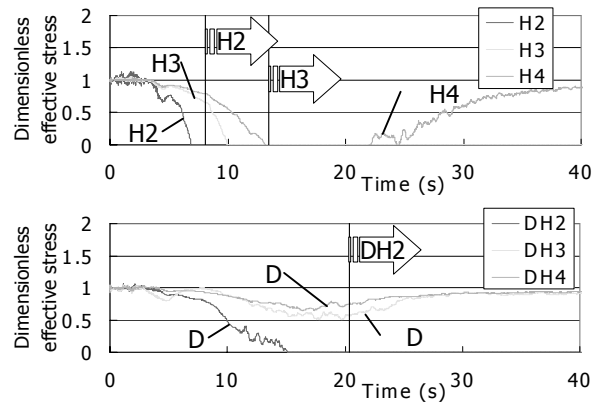


Fig. 9 Dimensionless effective stress impermeable structure

of other points, even if the liquefaction was not observed, the reduction of the effective stress is noticeable.

3.4 FINAL SCOUR DEPTH

The final scour depth is presented in Fig. 10 and Fig. 11 for permeable-structure and impermeable-structure case respectively. The scour hole is the deepest near the edge of the upstream-sidewall and the headwall. Maximum scour depth observed after the experiment equals 8.2 cm (permeable dike) and 9.9 cm (impermeable dike). Generally speaking scour hole has similar shape - the shape of a cone, but all the depths after the permeable-structure experiments are smaller. Also one can see in the graphs that the range of scouring is smaller. Sand washed out near the spur dike is deposited in the area sheltered by the dike.

Change of the sand level in time may be seen in Fig. 12 and Fig. 13. The observed scouring during the surge was different from what was described in the literature by Elawady (2001) and what was observed in a former research for the case of a stable flow. For the stable flow, the scouring was very intense at the start, and then gradually became weaker. The total scouring process lasted for a very long time. For the surge, during the whole time, when scouring took place, the process was characterized by equal intensity. The fading of the scouring intensity in time, described in the references for stable flow was not observed during the experiment with the surge.

The scouring starts about 3 to 4 seconds after opening the gate at the upstream sidewall - headwall corner. In columns where pressure was measured the scouring actions began after 5.2 seconds in the permeable-dike case and 4.7 seconds in the impermeable-dike case. The scouring action was very intensive and finished after about 25 seconds (for both cases). In both cases, in column H, the final scouring depth was shallower than what was recorded during the experiment. The difference between maximum and final scouring depth in both cases equaled up to 1 cm.

3.5 SEEPAGE FORCE

Figures 12 and 13 present pressure levels on the walls of the dike. The dark areas in those figures represent regions where the pressure was lowest. In case of impermeable structure, the pressure configuration at the sidewalls and headwall of the spur dike suggests water flow in the ground in directions marked by arrows in the figures. According to the pressure gradients, the seepage water flowed horizontally and upward from the upstream side area to the downstream side area. In the case of permeable structure, this pattern was not observed. Pressure gradient in this case is visible in the border between points in the sand and in the water. Inside the sand layer the pressure difference between points is negligibly small.

For the impermeable-structure case, the liquefaction process in the direct vicinity of the headwall and downstream sidewall described above enabled the flow out of the ground water. The seepage force was acting on the sand grains in the liquefied area promoting scouring process by water flow.

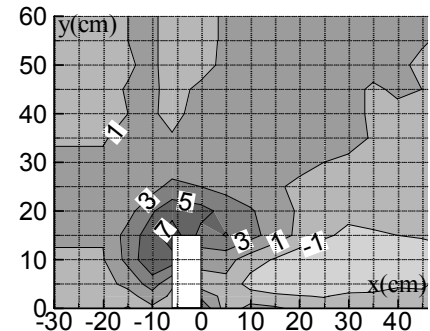


Fig. 10 Final scour depth (unit: cm) permeable structure

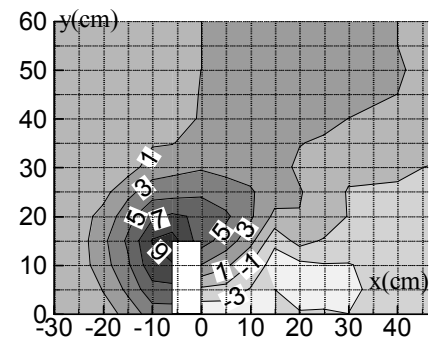


Fig. 11 Final scour depth (unit: cm) impermeable structure

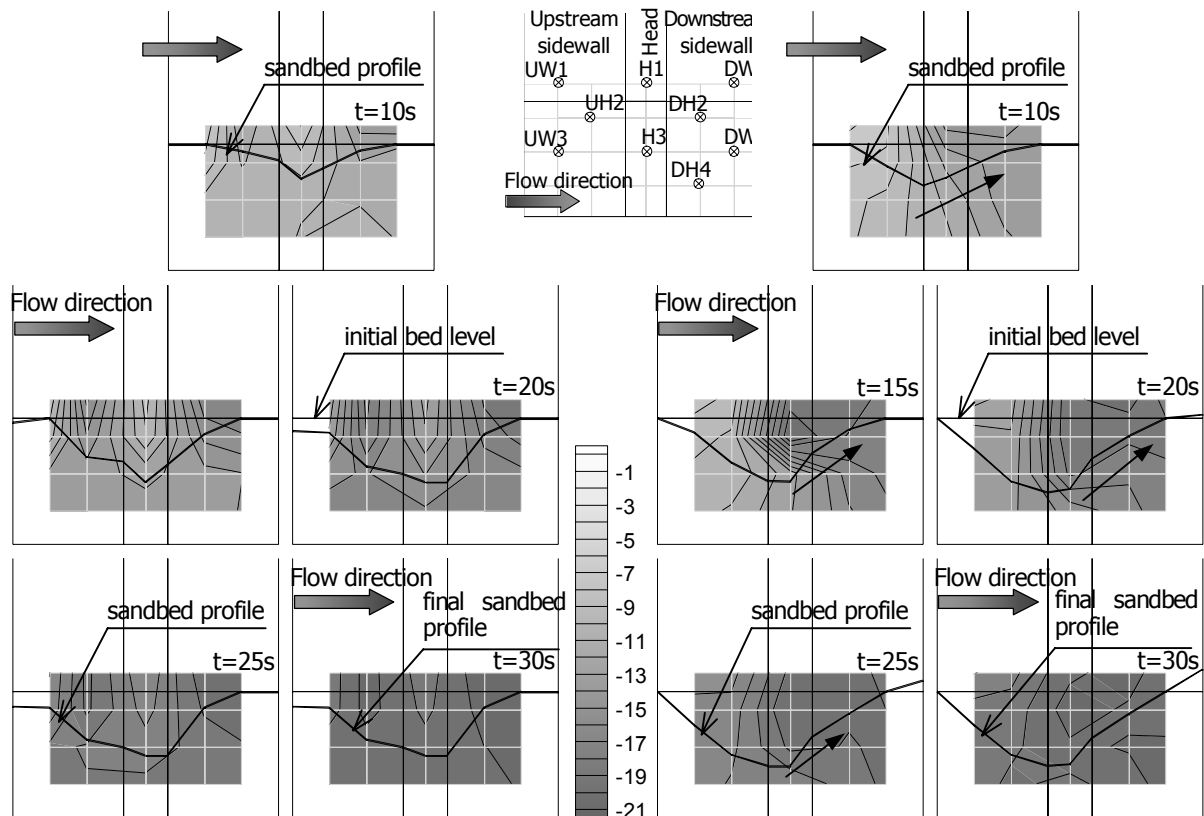


Fig. 12 Pressure on the spur dike walls and sandbed profile during the experiment – permeable structure

Fig. 13 Pressure on the spur dike walls and sandbed profile during the experiment – impermeable structure

4. CONCLUSIONS

Performed experiment proved the influence of structure permeability on flow pattern and phenomena in the vicinity of the spur dike. Permeability of the structure results in smaller intensity of processes that occur near the spur dike. In this context the scouring action, flux redirecting and excess pore water pressure has to be mentioned. Some of the phenomena observed in the case of impermeable structure i.e. seepage force was not seen in the case of permeable structure. Nevertheless, more detailed theoretical work and numerical simulations, especially of the storm surge or big waves which are the reason for many unexpected processes, are scheduled to be done in order to improve the knowledge of these phenomena. Their simulation will enable researchers to understand and analyze it in detail which is the main aim of this research.

REFERENCES

- Elawady, E., Michiue, M. and Hinokidani, O.: Experimental Study of Flow Behavior Around Submerged Spur-Dike on Rigid Bed, *Annual Journal of Hydraulic Engineering, JSCE*, vol. 44, pp. 539-544, 2000.
- Elawady, E., Michiue, M. and Hinokidani, O.: Movable Bed Scour Around Submerged Spur-Dikes, *Annual Journal of Hydraulic Engineering, JSCE*, vol. 45, pp. 373-378, 2001.
- Mia F. Sand Bed Behavior Under Water Pressure Variation and Local Scour at Bridge Piers, *Doctors Thesis*, Okayama University, 2002.
- Maeno, S., Magda, W., Nago, H.: Floatation of Buried Submarine Pipeline under Cyclic Loading of Water Pressure, *Proceedings of the Ninth International Offshore and Polar Engineering Conference*, Brest France, pp. 217-225, 1999.
- Nago, H.: Liquefaction of Highly Saturated Sand Layer under Oscilating Water Pressure, *Memoirs of the School of Engineering*, Okayama University, 1981

- Rahman, M., Murata, H., Nagata, N., Muramoto, Y.: Local Scour Around Spur-Dike-like Structures and their Countermeasures Using Sacrificial Piles, *Annual Journal of Hydraulic Engineering, JSCE*, vol. 42, pp. 991-996, 1998.
- Sumer B.M., Whitehouse J.S., Torum A.: Scour Around Coastal Structures: a summary of recent research, *Coastal Engineering*, vol. 44 pp. 153-190, 2001.
- Sumer B.M., Fredsoe J., Christiansen N., Hansen S.B.: Bed Shear Stress and Scour Around Coastal Structures, *Proceedings of 24th International Coastal Engineering Conference ASCE*, Kobe, Japan, vol. 2, pp. 1595-1609, 1994.